

# The Influence of the Gravure Printing Quality on the Layer Functionality: The Study Case of LFP Cathode for Li-Ion Batteries

Maria Montanino <sup>1,\*</sup>, Claudia Paoletti <sup>2</sup>, Anna De Girolamo Del Mauro <sup>1</sup> and Giuliano Sico <sup>1</sup>

<sup>1</sup> ENEA Italian National Agency for New Technologies, Energy and Sustainable Economic Development, Portici Research Centre, 80055 Portici, Italy; anna.degirolamo@enea.it (A.D.G.D.M.); giuliano.sico@enea.it (G.S.)

<sup>2</sup> ENEA Italian National Agency for New Technologies, Energy and Sustainable Economic Development, Casaccia Research Centre, 00123 Roma, Italy; claudia.paoletti@enea.it

\* Correspondence: maria.montanino@enea.it

**Abstract:** In light of the growing interest in printed batteries, we recently demonstrated the possibility of employing industrial gravure printing in battery manufacturing. Gravure is the most appealing printing technique for the low-cost production of functional layers, but it is rarely investigated since the necessity to use diluted inks makes it difficult to obtain proper functionality, especially in the case of composites, and an adequate mass loading of the printed layer. For this reason, the ink formulation represents one of the main challenges; ruling on it could strongly boost the use of such a technique in industrial manufacturing. It is known that a viable method for obtaining good gravure printing quality is based on the Capillary number approaching unity. Taking into account such methods for the choice of ink and the process parameters, here a study of the printing quality influence on the functionality and the performances of the gravure printed layer is proposed in the case of an LFP-based cathode for Li-ion batteries. Good printing quality is necessary to obtain proper layer functionality, but specific parameters have to be considered for achieving high performance.

**Keywords:** lithium batteries; printed electrodes; printed batteries; printing quality; gravure printing; Capillary number



**Citation:** Montanino, M.; Paoletti, C.; De Girolamo Del Mauro, A.; Sico, G. The Influence of the Gravure Printing Quality on the Layer Functionality: The Study Case of LFP Cathode for Li-Ion Batteries. *Coatings* **2023**, *13*, 1214. <https://doi.org/10.3390/coatings13071214>

Academic Editor: Octavian Buiu

Received: 31 May 2023

Revised: 28 June 2023

Accepted: 5 July 2023

Published: 6 July 2023



**Copyright:** © 2023 by the authors. Licensee MDPI, Basel, Switzerland. This article is an open access article distributed under the terms and conditions of the Creative Commons Attribution (CC BY) license (<https://creativecommons.org/licenses/by/4.0/>).

## 1. Introduction

Printed batteries are more and more investigated thanks to their small size (volume below 10 mm<sup>3</sup>), which makes them particularly suitable for portable and wearable electronics, biomedical devices, and the emerging internet of things (IoT) [1,2]. In fact, such batteries are able to respond to the most recent needs of miniaturization, integration, high customizability, and cost-effective production. In particular, the printed batteries can be produced in thin film form, also in a single in-line process, by the overlap of different layers, without any problem of alignment compared with other manufacturing processes, thanks to the automatic register. In perspective, the integration and perfect fitting of the batteries and different devices to be fed can be obtained by the same production process thanks to the versatility of the printing, which is appealing for the manufacturing of all the layered devices such as electronics. Such thin batteries are suitable for folding and rolling, appearing particularly appropriate for smart dust applications [3,4]. Recently, such growing interest motivated our studies on the use of gravure printing for the manufacturing of printed batteries.

Among the traditional printing techniques, gravure is considered the most attractive for low-cost functional layer production because of its unique capability to couple high speed (up to 400 m/min) and high resolution (below 2 μm), even in large-area printing [5–7]. Despite its many advantages, gravure printing is rarely investigated. One of the main challenges is the necessity to use highly diluted inks (<100 mPa s), which makes the achievement of proper functionality and/or an adequate mass loading of the printed layer difficult, especially in the case of composites as the electrodes [1,8].

Moreover, changing a component of the ink implies that a new formulation has to be investigated in terms of preparation and process parameters.

In our previous studies, we demonstrated the possibility of obtaining gravure printed electrodes for Li-ion batteries showing very good performances in terms of specific capacity, stability, and long-life cyclability [9–11]. Moreover, we developed a methodology, mainly based on the dimensionless Capillary number approaching unity, as a driver for the ink formulation and the choice of process parameters [12]. The Capillary number is related to the ink viscosity, surface tension, and printing speed; when this number approaches unity, good printing quality is typically achieved [7]. Here, a study on the correlation of the printing quality with the functionality of the gravure printed layer is proposed. For such an investigation, gravure-printed cathodes based on Lithium Iron Phosphate (LFP) were selected since they are widely used, investigated, and stable.

## 2. Materials and Methods

The inks were prepared using the following materials at a fixed weight percentage as dry content: LFP by Sud Chemie as active material (88%), sodium Carboxy Methyl Cellulose (CMC) by Panreac Quimica as binder (6%), and super P by Thermofisher as conductive carbon (6%). A mixture of demineralized water and 2-propanol (IPA, by Sigma Aldrich, St. Louis, MI, USA) (80/20 wt/wt%) was used as a solvent. Ball milling was introduced in the ink preparation to improve the mixing and material distribution using a short treatment time (5 min) in order to limit the LFP particle size and functionality decrease. The rheological behavior of the inks was analyzed by a rotational rheometer (by Haake, Waltham, Massachusetts, USA) at 25 °C in a range of shear rates of 1–2000 s<sup>-1</sup>. The inks were gravure printed on aluminum foils (thickness of 15 µm, by Sigma-Aldrich) using an IGT G1-5 printer equipped with a cylinder having a line density of 40 lines/cm, a stylus angle of 120°, a cell depth of 72 µm, and a screen angle of 53°. A multilayer approach was adopted to obtain a mass loading suitable for printed batteries by overlapping ten layers of the same ink. In fact, preliminary printing tests were performed to evaluate the number of layers suitable to obtain a mass loading adequate for practical use (about 1.5 mg/cm<sup>2</sup>, fixed as the target). After each printed layer, a fast drying using nitrogen was performed, while the final multilayer was dried at 100 °C for one hour. The printed cathodes were characterized through scanning electron microscopy (SEM, 1530, LEO Elektronenmikroskopie GmbH, Oberkochen, Germany), a digital micrometer (by Mitutoyo, Neuss, Germany), and tested in batteries versus lithium metal through charge and discharge cycles at constant and variable rates by Maccor equipment, using as electrolyte 1 M LiPF<sub>6</sub> in a 3:7 (wt:wt) mixture of ethylene carbonate (EC) and diethyl carbonate (DEC).

## 3. Results and Discussion

Gravure printing consists of direct low-viscosity ink transfer from separate engraved microcells of a chromed cylinder onto a substrate by the pressure of a counter cylinder, as depicted in Figure 1 [13,14].

Several parameters come into play in determining the final quality of the printed layer: the physical ones of the ink (viscosity, rheological behavior, surface tension, solvent evaporation rate) and of the substrate (surface energy, porosity, smoothness), together with those of the process (cell geometry and density, printing force and speed) [7,15].

The gravure printing process can be seen as a sequence of sub-processes, as follows: inking, for the ink microcells filling; doctoring, for removing the excessive ink from the non-engraved areas of the printing cylinder by means of a blade; transfer, for transferring ink onto the substrate by the pressure of a counter cylinder; spreading, when single ink droplets coalesce on the substrate, forming a continuous film; drying, when the solvent is removed from the film [13]. Each of such sub-processes has its own ideal operating regime, which corresponds to the final material arrangement in the printed layer [6].

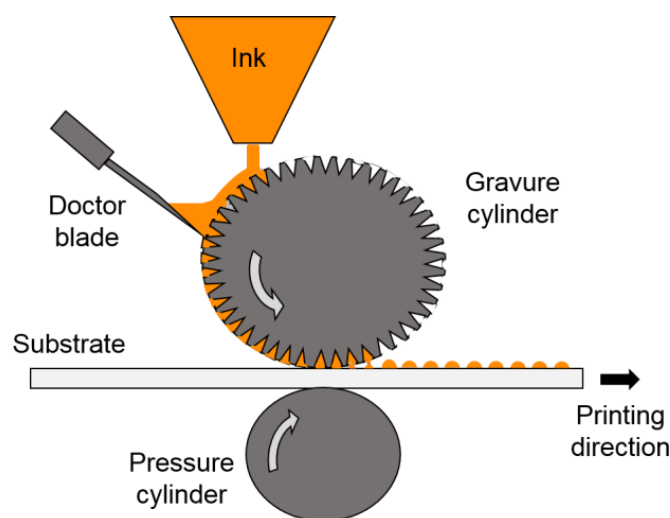


**Figure 1.** Schematic of the gravure printing process. Adapted with permission from Ref. [14].

Although it may seem like a relatively simple process, gravure printing has a complex multi-physical nature, involving capillarity, viscoelasticity, inertia, gravity, moving contact lines, and solvent evaporation changing ink composition, which makes modeling extremely challenging [6,16,17]. Since many different physical quantities are involved, dimensional analysis is typically used to simplify the complex gravure printing process, representing a useful tool for describing the physical system's behavior. At the microscopic level, the process fluid dynamics can be essentially reduced to the balance between viscous and surface tension forces, where the latter are the driving forces for the ink flow [6,18]. As a result, such a balance controls the printed pattern's morphology and fidelity [7]. At a particular printing speed ( $U$ ), the Capillary number represents the dimensionless number giving the strength of viscous forces over surface tension ones, as  $Ca = \eta U / \gamma$ , where  $\eta$  and  $\gamma$  are the viscosity and the surface tension of the ink, respectively [6,19,20]. Each gravure printing sub-process can display different dependencies on  $Ca$ , thus producing different regimes [6]. At low  $Ca$ , the pattern fidelity can be degraded by the ink drag-out from the cells, while at high  $Ca$ , ineffective doctoring can leave the ink in the non-engraved areas. Typically, the optimal compromise is achieved by adjusting the ink parameters and the printing speed to attain a  $Ca \approx 1$ , but deviations could be considered since the final printing quality depends on the complicated interplay of all the involved parameters [6,7,13,21]. However, it is not obvious that such a fluid-dynamic criterion of graphic print quality can simply be applied to functional materials for the fabrication of functional layers.

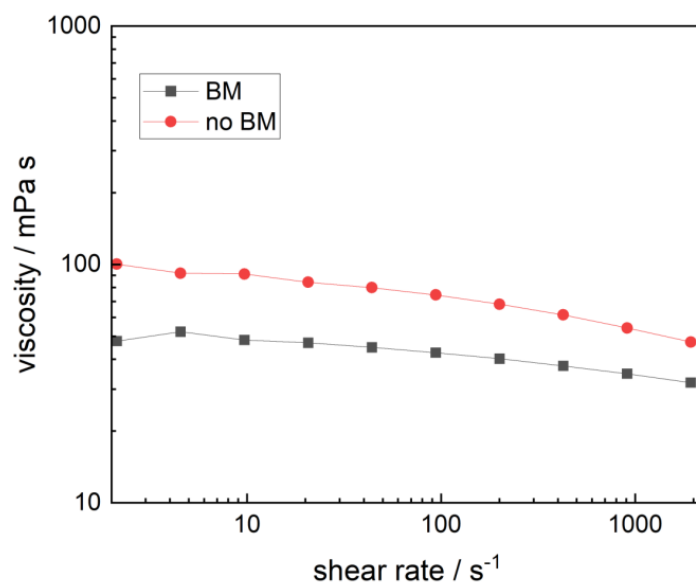
Here, an investigation of the influence of the printing quality on the layer functionality is proposed for functional printing of LFP-based cathodes for Li-ion batteries. Namely, using  $Ca$  approach unity as a method for both the ink formulation and printing process, the functional assessment of the gravure printed cathodes is discussed.

Electrode ink formulation has to contain specific components in an appropriate ratio: an active material (LFP), an electrical conductor (super P), and a binder (CMC). In particular, the binder was selected to be soluble in water; in this way, water can be used as the main solvent for improving the sustainability of electrode production. To obtain ink printability, 2-propanol was considered a co-solvent for decreasing the high water surface tension, making the surface tension of the ink lower than the surface tension of the substrate and of the printing cylinder [22,23]. Moreover, to meet the gravure printing requirements, the ink viscosity has to be lower than 100 mPa s; consequently, different ink solid contents were tested, changing also the preparation method as reported in Table 1. In particular, short-time ball milling was used to improve the mixing of the materials. The surface tension of all the prepared inks was considered the solvent one, and it was about 30 mN/m [24].

**Table 1.** Prepared ink characteristics.

Dry Solid Content [wt%]	Ball Milling	Viscosity [mPa s]
23	No	245
18	No	196
15	No	74
15	Yes	43
8	No	17

The inks having a solid content of 15 wt% fulfilled the gravure ink requirements and were gravure printed on aluminum foils overlapping ten layers of the same ink to reach an adequate mass loading for cathodic practical use. The viscosity values, reported in Table 1, were obtained by the rheological measurements considering the viscosity values at shear rate  $100 \text{ s}^{-1}$ ; such values were used for the Capillary number calculation since the rheological behavior of the tested inks was considered Newtonian, as shown in Figure 2. It is evident that the short-time ball-milled ink has a viscosity lower than the non-ball-milled ink, probably due to the decrease in large particle size, which improves particle flow and packing.

**Figure 2.** Viscosity versus shear rate for the 15 wt% not ball milled (no BM) and ball milled (BM) inks at 25 °C.

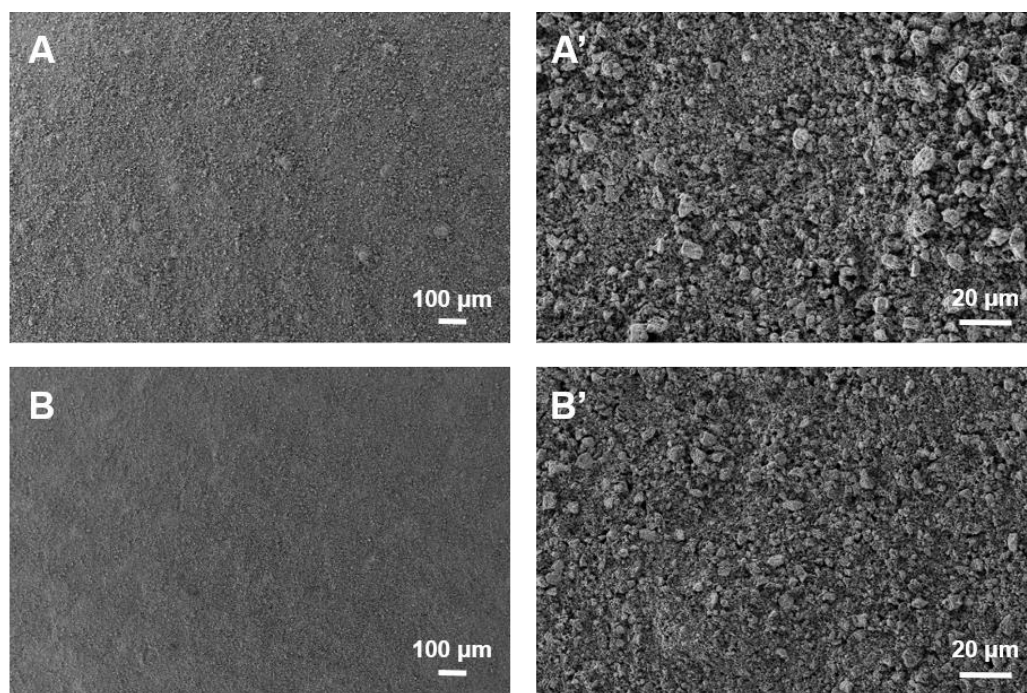
To determine the proper printing speed for obtaining a Ca approaching unity, calculations for the selected inks were made as reported in Table 2. Aiming to compare ball milled and not ball milled samples, only the cases in which Ca was closer to 1 were characterized, as reported in Table 2, where the characteristics refer to the overall printed layers (namely 10 overlapped layers). Printing tests were carried out to find the best printing force and the suitable number of overlapped layers to obtain both an appropriate mass loading (about  $1.5 \text{ mg/cm}^2$ ) and the absence of macroscopic defects.

In Figure 3, the SEM images of the investigated printed cathodes are reported. In both cases, the samples showed high quality, namely, without visible defects, very good coverage, and high uniformity in the material distribution. When the ink is ball milled, a slight decrease in the particle dimension is evident on the top surface of the printed layers. The gravure-printed cathodes were finally tested in half-cell vs. Lithium metal.



**Table 2.** Printing parameters and printed layer characteristics.

Dry Solid Content [wt%]	Ball Milling	Printing Speed [m/min]	Printing Force [N]	Ca	Mass Loading [mg/cm <sup>2</sup> ]	Layer Thickness [μm]	Apparent Layer Density [g/cm <sup>3</sup> ]
15	No	12	700	0.5			
15	Yes	12	700	0.3			
15	No	36	700	1.5	1.8 ± 0.2	20 ± 1	0.90
15	Yes	36	700	0.8	1.4 ± 0.2	15 ± 1	0.93
15	No	60	700	2.4			
15	Yes	60	700	1.4			

**Figure 3.** Top surface of the gravure-printed cathodes by non-ball-milled (A,A') and ball-milled (B,B') ink.

The electrochemical characterization of the printed cathodes is reported in Figure 4 at a constant and variable rate, respectively, for both samples. As it can be seen, the performances display good functionality of the printed layers; in particular, the specific capacity of the printed cathode obtained by the ball-milled ink is very close to the theoretical value (170 mAh g<sup>-1</sup>), while the printed cathode obtained by the non-ball-milled ink shows a slightly lower specific capacity, especially at high rates. Probably, this is due to the effect of the short ball-milling time that slightly decreases the active material particle size, increasing its surface/volume ratio, and improving the interconnection among the components at such a fixed percentage. On the basis of the theoretical density of each component, the porosity of the electrodes was estimated at 38% for the layer printed using non-ball-milled ink and at 36% for the layer printed using ball-milled ink. The very good properties obtained through the gravure printing allow to skip the calendaring step in the electrode manufacturing process, which instead is necessary when typical casting/coating processes are used.

Therefore, the methodology based on Ca for the ink formulation and the printing process is a very good driver for obtaining good gravure printing quality. The high printing quality is a necessary condition for the layer functionality but is not sufficient to guarantee a high functional quality, which is influenced by additional specific parameters, as in the case of printed batteries, where the contribution of mass loading, component ratio, component distribution, and layer density plays an important role. When all the conditions are respected, very good performances are achieved; in fact, for the electrodes, a long cycle life is obtained, cycling at high and constant capacity without fading for a long number of cycles [10]. This is due to the high homogeneity and lack of defects in the printed layers, which avoid preferential accumulation during the charge and discharge processes

and preventing local degradation and dendrite formation. It is expected that such good results can also be achieved in the study of other storage systems, especially in the case of large-area devices.

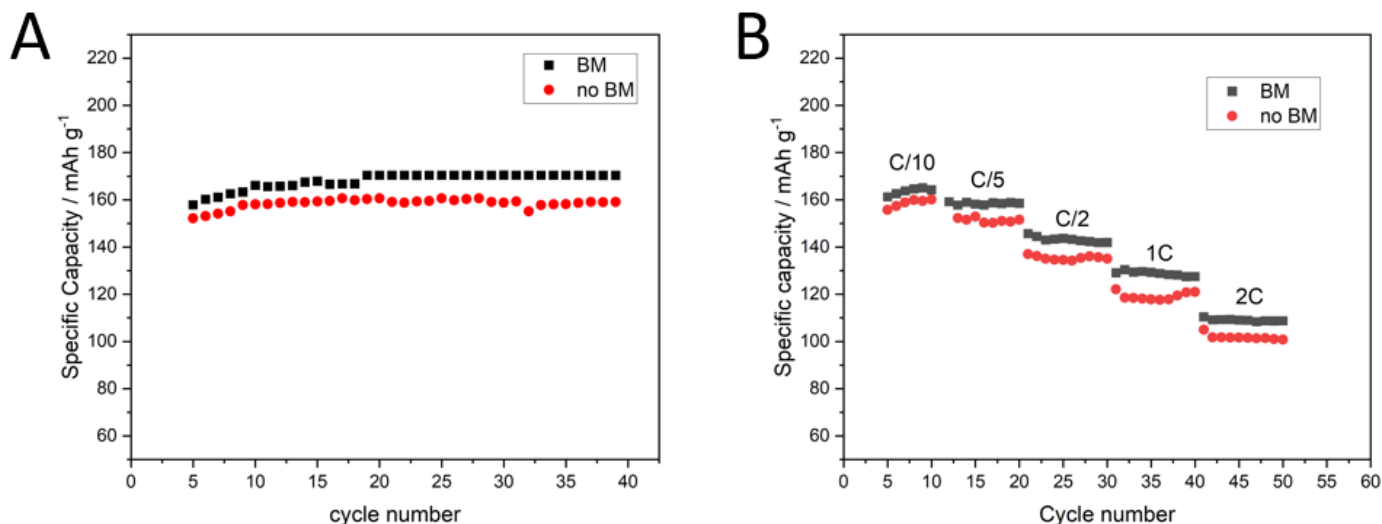


**Figure 4.** Discharge specific capacity versus cycle number for the gravure printed cathodes by non-ball-milled (no BM) and ball-milled (BM) ink at a constant C/10 rate (A) and variable rate (B).

The obtained results can be considered useful for the gravure printing of different functional layers since they validate a method for obtaining good printing quality, thus enabling specific layer functionality. However, every single time the system, the application, and the involved materials change, a specific study is necessary to achieve high performances in order to keep into account specific parameters and challenges that play a fundamental role in each considered case.

#### 4. Conclusions

In this paper, a methodology based on Ca for obtaining a high-quality gravure printed layer is discussed in the specific case of printed batteries. The experiments showed that the choice of ink and process parameters for Ca approaching unity is a good driver to provide a good printing quality able to guarantee the proper functionality of the printed layer. Nevertheless, such a condition is not sufficient to obtain high-quality performances, depending on the specific parameters that come into play for each specific functionality. In this case, ink ball-milling was able to improve the electrochemical performances of the gravure-printed cathodes owing to its ability to improve the material distribution and the interplay of components. Such a study case of an LFP printed cathode can serve as a model for extending the obtained results to other electrodes, including anodes, based on different active materials, e.g., graphite or lithium transition metal oxides, for which the methodology for inks and processes and the boundary conditions are similar. Such a study provides an important improvement in the process knowledge devoted to gravure printing functional layer production and represents a further boost for the future low-cost industrial use of gravure printing in the field of printed batteries.

**Author Contributions:** Conceptualization, M.M. and G.S.; methodology, M.M. and G.S.; validation, M.M., A.D.G.D.M., C.P. and G.S.; investigation, M.M., A.D.G.D.M., C.P. and G.S.; resources, M.M. and C.P.; data curation, M.M., C.P. and G.S.; writing—original draft preparation, M.M.; writing—review and editing, M.M. and G.S.; visualization, M.M., A.D.G.D.M., C.P. and G.S.; supervision, M.M. and G.S.; funding acquisition, M.M. All authors have read and agreed to the published version of the manuscript.

**Funding:** This work was partially supported by Accordo di Programma MiTe-ENEA 2021–2024 Mission Innovation (CUP I62C21000380001) WP2-Materiali sostenibili per accumulo elettrochimico dell'energia and partially supported by Accordo di Programma 2022–2024 Progetto di ricerca integrato: Tecnologie di accumulo elettrochimico e termico (CUP I53C22003080001) WP1- Accumulo elettrochimico: materiali avanzati.

**Institutional Review Board Statement:** Not applicable.

**Informed Consent Statement:** Not applicable.

**Data Availability Statement:** The raw data can be obtained from the corresponding authors upon reasonable request.

**Conflicts of Interest:** The authors declare no conflict of interest.

## References

1. Oliveira, J.; Costa, C.M.; Lanceros-Méndez, S. *Printed Batteries Materials, Technologies and Applications*; John Wiley & Sons Ltd.: Chichester, UK, 2018.
2. Costa, C.M.; Gonçalves, R.; Lanceros-Méndez, S. Recent advances and future challenges in printed batteries. *Energy Storage Mater.* **2020**, *28*, 216–234. [[CrossRef](#)]
3. Zhu, M.; Shmidt, O.G. Tiny robots and sensors need tiny batteries—Here's how to do it. *Nature* **2021**, *589*, 195. [[CrossRef](#)] [[PubMed](#)]
4. You, C.-Y.; Hu, B.-F.; Xu, B.-R.; Zhang, Z.-Y.; Wu, B.-M.; Huang, G.-S.; Song, E.-M.; Mei, Y.-F. Foldable-circuit-enabled miniaturized multifunctional sensor for smart digital dust. *Chip* **2022**, *1*, 100034. [[CrossRef](#)]
5. Grau, G.; Kitsomboonloha, R.; Subramanian, V. Fabrication of a high-resolution roll for gravure printing of 2 $\mu$ m features. In Proceedings of the SPIE Organic Photonics + Electronics, San Diego, CA, USA, 9–13 August 2015.
6. Grau, G.; Subramanian, V. Fully High-Speed Gravure Printed, Low-Variability, High-Performance Organic Polymer Transistors with Sub-5 V Operation. *Adv. Electron. Mater.* **2016**, *2*, 1500328. [[CrossRef](#)]
7. Huang, Q.; Zhu, Y. Printed Electronics: Printing Conductive Nanomaterials for Flexible and Stretchable Electronics: A Review of Materials, Processes, and Applications. *Adv. Mater. Technol.* **2019**, *4*, 1800546. [[CrossRef](#)]
8. Hwang, S.S.; Cho, C.G.; Park, K.-S. Stabilizing LiCoO<sub>2</sub> electrode with an overlayer of LiNi<sub>0.5</sub>Mn<sub>1.5</sub>O<sub>4</sub> by using a Gravure printing method. *Electrochem. Commun.* **2011**, *13*, 279–283. [[CrossRef](#)]
9. Montanino, M.; Sico, G.; De Girolamo Del Mauro, A.; Moreno, M. LFP-Based Gravure Printed Cathodes for Lithium-Ion Printed Batteries. *Membranes* **2019**, *9*, 71. [[CrossRef](#)] [[PubMed](#)]
10. Montanino, M.; Sico, G.; De Girolamo Del Mauro, A.; Asenbauer, J.; Binder, J.R.; Bresser, D.; Passerini, S. Gravure-Printed Conversion/Alloying Anodes for Lithium-Ion Batteries. *Energy Technol.* **2021**, *9*, 2100315. [[CrossRef](#)]
11. Montanino, M.; De Girolamo Del Mauro, A.; Paoletti, C.; Sico, G. Gravure Printing of Graphite-Based Anodes for Lithium-Ion Printed Batteries. *Membranes* **2022**, *12*, 999. [[CrossRef](#)] [[PubMed](#)]
12. Montanino, M.; Paoletti, C.; De Girolamo Del Mauro, A.; Sico, G. Gravure printed composites based on Lithium Manganese Oxide: A study case for Li-ion batteries manufacturing. *Macromolecular Symposia*; submitted.
13. Sico, G.; Montanino, M.; Prontera, C.T.; De Girolamo Del Mauro, A.; Minarini, C. Gravure printing for thin film ceramics manufacturing from nanoparticles. *Ceram. Int.* **2018**, *44*, 19526–19534. [[CrossRef](#)]
14. Garcia, A.J.L.; Sico, G.; Montanino, M.; Defoor, V.; Pusty, M.; Mescot, X.; Loffredo, F.; Villani, F.; Nenna, G.; Ardila, G. Low-Temperature Growth of ZnO Nanowires from Gravure-Printed ZnO Nanoparticle Seed Layers for Flexible Piezoelectric Devices. *Nanomaterials* **2021**, *11*, 1430. [[CrossRef](#)]
15. Khan, S.; Lorenzelli, L.; Dahiya, R.S. Technologies for printing sensors and electronics over large flexible substrates: A review. *IEEE Sens. J.* **2014**, *15*, 3164–3185. [[CrossRef](#)]
16. Khandavalli, S.; Rothstein, J.P. Ink transfer of non-Newtonian fluids from an idealized gravure cell: The effect of shear and extensional deformation. *J. Non-Newton. Fluid Mech.* **2017**, *243*, 16–26. [[CrossRef](#)]
17. Pingulkar, H.; Peixinho, J.; Crumeyrolle, O. Liquid transfer for viscoelastic solutions. *Langmuir* **2021**, *37*, 10348–10353. [[CrossRef](#)]
18. Choi, Y.; Kim, G.H.; Jeong, W.H.; Kim, H.J.; Chin, B.D.; Yu, J.-W. Characteristics of gravure printed InGaZnO thin films as an active channel layer in thin film transistors. *Thin Solid Film* **2010**, *518*, 6249–6252. [[CrossRef](#)]
19. Sankaran, A.K.; Rothstein, J.P. Effect of viscoelasticity on liquid transfer during gravure printing. *J. Non-Newton. Fluid Mech.* **2012**, *175*, 64–75. [[CrossRef](#)]
20. Liang, J.; Jiang, C.; Wu, W. Printed flexible supercapacitor: Ink formulation, printable electrode materials and applications. *Appl. Phys. Rev.* **2021**, *8*, 021319. [[CrossRef](#)]
21. Sico, G.; Montanino, M.; Loffredo, F.; Borriello, C.; Miscioscia, R. Gravure Printing for PVDF Thin-Film Pyroelectric Device Manufacture. *Coatings* **2022**, *12*, 1020. [[CrossRef](#)]
22. Glasser, A.; Cloutet, E.; Hadziioannou, G.; Kellay, H. Tuning the rheology of conduction polymer inks for various deposition processes. *Chem. Mater.* **2019**, *31*, 6936–6944. [[CrossRef](#)]

23. Chang, Q.; Cao, C.; Qiao, H.; Hu, Y.; Xiao, G.; Shi, W. Ink transfer for printed flexible microsupercapacitors. *Carbon* **2021**, *178*, 285–293. [[CrossRef](#)]
24. Vázquez, G.; Alvarez, E.; Navaza, J.M. Surface Tension of Alcohol + Water from 20 to 50 °C. *J. Chem. Eng. Data* **1995**, *40*, 611–614. [[CrossRef](#)]

**Disclaimer/Publisher’s Note:** The statements, opinions and data contained in all publications are solely those of the individual author(s) and contributor(s) and not of MDPI and/or the editor(s). MDPI and/or the editor(s) disclaim responsibility for any injury to people or property resulting from any ideas, methods, instructions or products referred to in the content.